

PAPER

Identifying genes associated with phenotypes using machine and deep learning

Muhammad Muneeb,^{1,2} David B. Ascher^{1,2,*} and YooChan Myung^{1,2}¹School of Chemistry and Molecular Biology, The University of Queensland, Queen Street, 4067, Queensland, Australia and²Computational Biology and Clinical Informatics, Baker Heart and Diabetes Institute, Commercial Road, 3004, Victoria, Australia

*Corresponding authors: David B. Ascher, Email: d.ascher@uq.edu.au

FOR PUBLISHER ONLY Received on Date Month Year; revised on Date Month Year; accepted on Date Month Year

Abstract

Identifying disease-associated genes enables the development of precision medicine and the understanding of biological processes. Genome-wide association studies (GWAS), gene expression data, biological pathway analysis, and protein network analysis are among the techniques used to identify causal genes. We propose a machine-learning (ML) and deep-learning (DL) pipeline to identify genes associated with a phenotype. The proposed pipeline consists of two interrelated processes. The first is classifying people into case/control based on the genotype data. The second is calculating feature importance to identify genes associated with a particular phenotype. We considered 30 phenotypes from the openSNP data for analysis, 21 ML algorithms, and 80 DL algorithms and variants. The best-performing ML and DL models, evaluated by the area under the curve (AUC), F1 score, and Matthews correlation coefficient (MCC), were used to identify important single-nucleotide polymorphisms (SNPs), and the identified SNPs were compared with the phenotype-associated SNPs from the GWAS Catalog. The mean per-phenotype gene identification ratio (GIR) was 0.84. These results suggest that SNPs selected by ML/DL algorithms that maximize classification performance can help prioritise phenotype-associated SNPs and genes, potentially supporting downstream studies aimed at understanding disease mechanisms and identifying candidate therapeutic targets.

Key words: bioinformatics, deep learning, gene identification, genome analysis, genetics, machine learning

Introduction

The interplay between genetic and environmental differences results in the variation in visual [1] (height) and non-visual characteristics [2] (behavior). Various environmental factors, such as diet, oxygen levels, and others, have been shown to influence many phenotypes directly [3, 4]. The degree to which these effects influence phenotypes is often influenced by subtle underlying genetic differences that can alter gene expression and biological processes [5].

The process of locating genes within a genome and determining their structure, function, and associations with specific traits or biological processes is known as gene identification [6, 7]. Several methods exist to identify genes associated with phenotypes, including genome-wide association studies (GWAS) [8], gene expression data analysis [9], biological pathways analysis [10], protein network data analysis [11], transcriptome-wide association studies [12] and machine learning methods [13, 14].

Traditionally, researchers use genome-wide association studies (GWAS) to identify SNPs that show strong associations with phenotypes. These association signals are then further investigated using approaches such as fine-mapping, gene expression analysis, colocalization studies, and biological

pathway analysis to refine and interpret the genetic associations. In this study, we adopt a different strategy by using ML/DL models for variant prioritisation. Our approach assumes that models with higher classification performance identify SNPs that better discriminate cases from controls and are therefore more likely to be associated with the phenotype [15, 14, 16]. We first performed association testing and p-value thresholding to construct reduced SNP sets and then trained ML/DL models for phenotype classification. Feature-importance methods are subsequently used to rank SNPs and prioritise genes contributing most to phenotype prediction.

The process by which information encoded in a gene is used to produce a functional product, such as RNA or protein, is known as gene expression. Gene expression data are measured using technologies such as microarrays or RNA sequencing, and genes associated with specific phenotypes can be identified using statistical methods such as differential gene expression analysis [17, 18, 19, 20]. Gene expression data are used for gene and biomarker identification in diseases such as colorectal cancer [21, 22], prostate cancer [23], brain cancer [24], bipolar disorder [25], and gastric cancer [26] using bioinformatics frameworks. Additional experiments or data sources are typically required to confirm and interpret the

biological relevance of the discovered genes, as gene expression data alone do not provide direct evidence of gene function [27].

GWAS has been widely used to identify SNPs associated with phenotypes and involves scanning individual SNPs and comparing allele frequencies between cases and controls [28, 29]. The process involves recruiting people exhibiting variation in the phenotype of interest and sequencing the genotype data. The next step is to improve genotype data quality by removing SNPs with low genotype rates. After that, association testing is performed on each SNP to identify whether a particular SNP shows a significant difference in the allele frequency between cases and controls [30], and this methodology has been used for gene identification in diseases such as blood pressure [31], Parkinson disease [32], and Alzheimer’s disease [33]. Because the identified variants (SNPs) have limited predictive value, they cannot provide a comprehensive understanding of the underlying biological mechanisms.

Machine learning methods like Random Forest and Gradient Boosting [34], Gradient Boosting Machine [35], and Support Vector Machine (SVM) [36] can be applied to association studies to evaluate the significance of SNPs in predicting phenotype status [13, 37]. These methods assess the usefulness of each SNP, and the SNP significance score can be used to order the SNPs and identify those of high importance [15]. These methods use permutation-based [38] and feature importance techniques to rank SNPs and have been applied to breast cancer [37], pancreatic cancer [39], cancer [40], and Alzheimer’s disease [41]. Moreover, feature selection approaches such as recursive feature elimination and the Least Absolute Shrinkage and Selection Operator (LASSO) regression can also be used to rank SNPs.

Machine learning algorithms have been used for gene function prediction [42], gene-gene interactions [43], and gene expression analysis [44]. In this study, we used machine learning to identify genes from genotype data.

Among methods that use genotype data for gene identification, GWAS and machine/deep learning are prominent, relying on SNPs to identify associated genes. Every gene is composed of multiple SNPs; identifying SNPs associated with a particular phenotype or trait results in identifying a gene associated with a phenotype [8]. Some SNP variations can modify gene expression, protein structure, or protein-protein interactions, thereby affecting functional outcomes and contributing to complex phenotypic features, including disease susceptibility and drug responsiveness, making them good candidates for gene identification.

We used ML and DL algorithms for genotype-phenotype prediction. Then, the best-performing model was used to rank the SNPs or features that contributed most to the separation of cases and controls, and the identified SNPs for each phenotype were compared with existing phenotype-associated SNPs from the GWAS Catalog. The proposed methodology was tested on 30 phenotypes from the openSNP data, and ML/DL algorithms identified genes (listed in the GWAS Catalog) associated with phenotypes.

Methodology

Modeling

We considered binary phenotypes from the openSNP data [45], and the dataset processing steps are explained in detail in the supplementary material (section 1). The following describes the process after genotype data conversion. Figure 1

shows the overall workflow of identifying genes associated with phenotypes using machine learning models.

Duplicate genotype files and SNPs were discarded, leaving 80 phenotypes. A list is available on GitHub (Analysis3.pdf). We considered a Hardy–Weinberg equilibrium threshold of 1×10^{-6} , a genotype missingness threshold of 0.01, a minor allele frequency threshold of 0.01, and an individual missingness threshold of 0.7 [46, 47] to improve genotype data quality.

We searched the GWAS Catalog for each phenotype and found SNP association data available for 36 phenotypes. The table showing the association study number for each phenotype is available on GitHub (Table1.md). Each phenotype has multiple association files, and we considered one association file with a high name resemblance to a specific phenotype. We downloaded the associations for each phenotype and checked whether these SNPs were present in the processed genotype data. Table 1 lists the phenotype, the number of associated SNPs from the GWAS Catalog, the number of SNPs in the genotype data for a particular phenotype, and the number of common SNPs between the GWAS Catalog and genotype data. Six phenotypes with no common SNPs were removed, leaving 30 for further analysis.

We used PLINK to split the data (stratified 5-fold) into training (80%) and test sets (20%), and we performed the following steps on each fold. The training data were subjected to Fisher’s exact test for allelic association (using `plink --assoc`) to generate the GWAS summary statistics, which contain p-values for each SNP. Using p-value thresholding, we extracted the top 50, 100, 200, 500, 1000, 5000, and 10000 SNPs from the training and test data and saved the encoded data in a raw tabular format for model training.

We considered multiple hyperparameters for the deep learning models, while we used the default hyperparameters for the machine learning models. We adjusted the hyperparameters of the deep learning models to obtain a new version of the model. We used AUC, F1 score, and MCC to assess the model’s performance. We averaged the AUC, F1 score, and MCC across all folds for each model to identify the best-performing model for each evaluation metric [48].

We listed the features from the models yielding the best AUC, F1 Score, and MCC for each phenotype. A single model that yields the best performance in terms of AUC may not necessarily yield the best performance in terms of MCC or F1 Score [49], and selecting multiple models optimized for different evaluation metrics helps identify the discriminative boundary between cases and controls and improves feature selection. We extracted the top-ranked SNPs from each model’s feature-importance method and compared them with SNPs and genes from the GWAS Catalog.

Implementation

This section provides implementation details of the ML/DL models and the feature importance process for both techniques, which affect gene identification.

Machine learning - models

We used 21 machine learning algorithms and their variants implemented in the `scikit-learn` library [50]. The algorithms include tree-based classification algorithms [51] (AdaBoost, XGBoost [52], Random Forest, and Gradient boosting algorithms), Stochastic Gradient Descent (SGD), Support Vector Classifier (SVC) [53], and other algorithms. The list

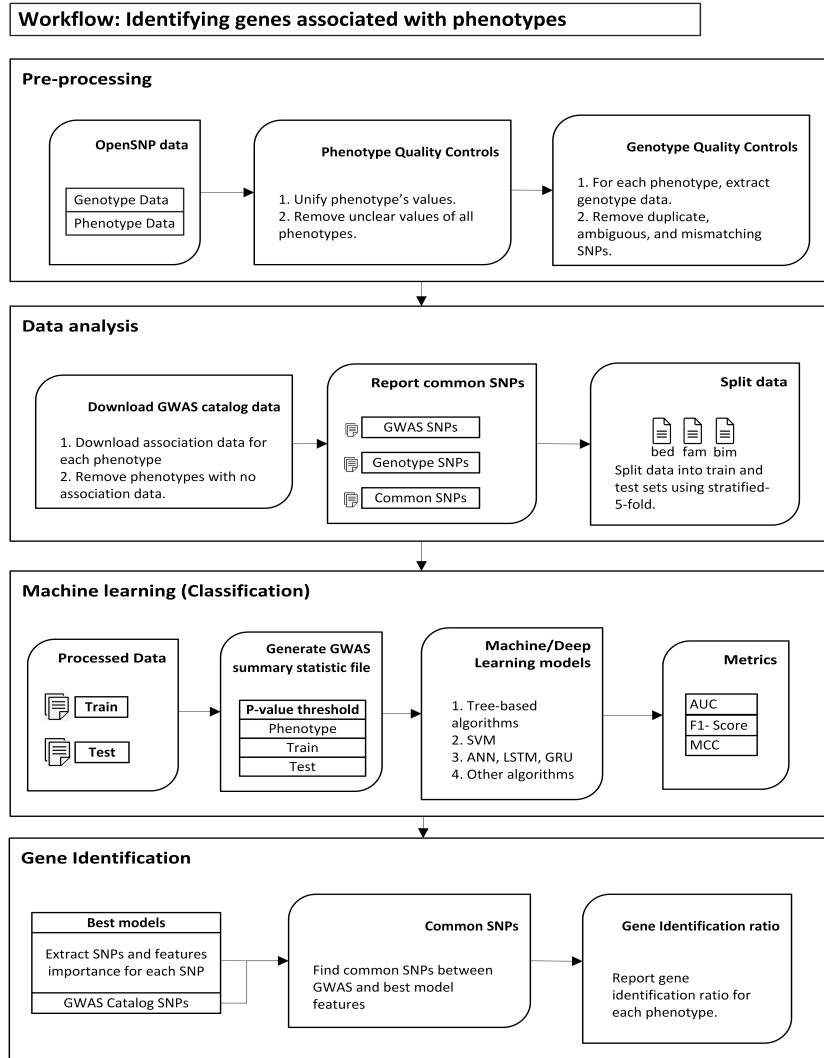


Fig. 1. A workflow of identifying genes associated with phenotypes. First, clean phenotype data, convert genotype data to PLINK format, and perform quality control steps on genotype data. Then, download gene associations for each phenotype. Split the data into five folds and generate bed, bim, and fam files for each split. Divide genotype data into training and test sets, generate sub-datasets using p-value thresholds, pass data to machine/deep learning models, and report AUC, MCC, and F1-Score for each model and p-value thresholds. Finally, list the feature (SNPs) importance for the best-performing models, compare the identified SNPs with those downloaded from the GWAS Catalog, and report the gene identification ratio for each phenotype.

of 21 machine-learning algorithms is available on GitHub (MachineLearningAlgorithms.txt).

To calculate feature importance for SVC and similar methods, extract the coefficients of the learned hyperplane, take the absolute values of the coefficients, normalize the coefficient values, and those values are feature importance for all the features used to train the machine learning algorithm [54]. Tree-based algorithms, such as Random Forest, compute feature importance by measuring how much impurity is reduced by splitting each feature. XGBoost computes feature importance as the number of times a feature is used in the boosting process and the magnitude of its contribution to the loss function [14, 55].

Deep learning - models

We used four deep learning models: Artificial neural network (ANN) [56], Gated recurrent unit (GRU) [57], Long Short-Term

Memory (LSTM) [58], and Bidirectional LSTM (BiLSTM) [59]. There were five layers in each model, and the numbers of neurons in each layer were $128 + \sqrt[3]{S}$, $64 + \sqrt[4]{S}$, $32 + \sqrt[5]{S}$, $16 + \sqrt[6]{S}$, and 1, where S is the number of SNPs in the genotype data. As genotype data contain different numbers of SNPs, the models adjust themselves to the input size, and using the root of the number of SNPs allows the same model to be trained on datasets of different dimensionality. We created six new stacked model architectures using GRU, LSTM, and BiLSTM layers. We generated 80 deep learning models by varying four hyperparameters, as shown in Table 2. This combination of hyperparameters yielded 8 distinct models of a specific architecture. The list of 80 deep learning algorithms is available on GitHub (DeepLearningAlgorithms.txt).

We used feature dropout to compute feature importance. First, train the model, evaluate baseline performance, iterate over each input feature individually, drop that feature, evaluate

Phenotype	SNPs in GWAS Catalog	SNPs in our data	Common SNPs
Attention Deficit Hyperactivity Disorder (ADHD)	1818	63900	42
Allergic rhinitis	399	102988	16
Amblyopia	15	101302	0
Asthma	3291	681937	408
Bipolar Disorder	1585	101478	66
Cholesterol	5000	69425	130
Cluster headache	6	102495	0
Craves sugar	85	104592	2
Dental decay	294	105383	24
Depression	2586	99857	82
Diagnosed Vitamin D deficiency	30	105035	4
Diagnosed with Sleep Apnea	73	101361	6
Dyslexia	126	104630	2
Earlobe Free or attached	201	100852	11
Eczema	505	104091	15
Generalized Anxiety Disorder	23	67828	0
Hair Type	21	687752	7
Have Myalgic Encephalomyelitis/Chronic Fatigue Syndrome (ME/CFS)	5	106221	0
Hypertension	688	73859	52
Hypertriglyceridemia	36	218086	4
Irritable Bowel Syndrome	34	105698	2
Mental Disease	4988	98153	180
Migraine	642	107740	25
Motion Sickness	35	71798	3
Panic Disorder	24	105010	2
Photoc sneeze reflex (photoptarmic reflex)	56	97380	4
Plantar fasciitis	2	106492	0
Post-Traumatic Stress Disorder (PTSD)	137	102913	5
Restless leg syndrome	64	100985	6
Scoliosis	1392	100822	29
Seborrheic Dermatitis	12	105299	0
Sensitivity to Mosquito Bites	434	103606	3
Sleep Disorders	4067	101291	93
Strabismus	30	101765	1
Thyroid Issues Cancer	92	101747	8
TypeIIIdiabetes	5000	100694	193

Table 1. Phenotypes and the number of overlapping SNPs between the genotype data and the GWAS Catalog. The table lists phenotypes and the number of SNPs shared between the GWAS Catalog and the genotype dataset. No overlapping SNPs were identified for six phenotypes (Amblyopia, Cluster headache, Generalized anxiety disorder, ME/CFS, Plantar fasciitis, and Seborrheic dermatitis); therefore, these phenotypes were excluded from further analysis.

Parameters	Values
Dropout	0.2,0.5
Optimizer	Adam
Batch size	1,5
Epochs number	50,200

Table 2. Deep learning model’s hyperparameters and values. The first column shows the deep learning model’s hyperparameters, and the second column shows the values we considered for each hyperparameter. The combination of hyperparameter values yielded 8 ($2 * 1 * 2 * 2$) models for a given architecture.

performance, record the change in performance relative to the baseline, and rank the dropped feature by the change in performance. A larger drop in performance suggests higher importance, while a small drop implies lower importance [60, 61, 62].

Once we identified all models that yielded the best performance on AUC, MCC, and F1 Score for a specific phenotype, we ranked SNPs by feature-dropout importance and compared the highest-ranked SNPs with GWAS Catalog associations. The process is explained in Figure 2.

Results

Classification performance of machine and deep learning models

Figure 3 shows the classification results for all phenotypes. The detailed results for the best-performing models, in terms of AUC, F1 Score, and MCC, for both ML and DL are provided in Supplementary Section 1.

Among machine learning algorithms, XGBoost and its variants achieved the highest AUCs, yielding the best results

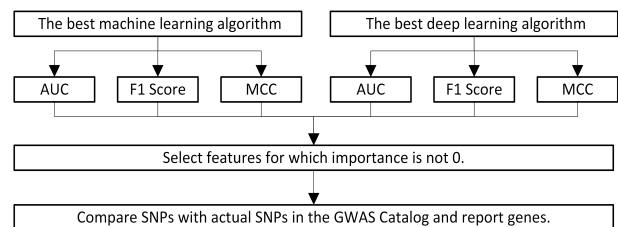


Fig. 2. A process of listing features identified by machine and deep learning models. We extracted the top-ranked SNPs from the best-performing machine and deep learning models in terms of AUC, F1 Score, and MCC. Those SNPs were compared with the actual SNPs from the GWAS Catalog.

for 18 phenotypes. The SGD classifier was the best-performing model for 15 phenotypes in terms of MCC and for 9 phenotypes in terms of F1 Score. Among deep learning algorithms, ANN performed best for most phenotypes across all evaluation metrics.

We calculated the average performance of ML/DL algorithms in terms of AUC, F1 Score, and MCC across all phenotypes. We found that deep learning algorithms achieved better performance on MCC and F1 Score, whereas machine learning achieved better performance on AUC, as shown in Table 3.

Gene Identification

We investigated the number of causal genes identified by the best-performing models. Figure 4 shows the number of genes identified for each phenotype when the best-performing ML/DL



Fig. 3. A heatmap showing the AUC, F1 score, and MCC for machine and deep learning. This heatmap shows the classification results from the best-performing models from the deep (DL) and machine (ML) learning algorithms in terms of AUC, F1 score, and MCC.

	Machine learning	Deep learning
AUC	0.65	0.63
F1 Score	0.53	0.54
MCC	0.24	0.28

Table 3. Average classification performance of machine- and deep-learning algorithms in terms of AUC, F1 score, and MCC. Performance for each metric was calculated as the mean across phenotypes, where each phenotype metric was averaged across cross-validation folds.

We calculated correlations between the best classification performance achieved by ML and DL models, measured using AUC, F1 score, and MCC, and the number of genes identified by the algorithms for each phenotype (Table 4). This analysis evaluates whether a particular model type (ML or DL) and evaluation metric (AUC, F1 score, or MCC) is associated with identifying a greater number of genes. The results indicate that deep-learning models optimized for MCC show a relatively stronger positive correlation, suggesting that optimizing MCC may be associated with identifying more genes than optimizing AUC or F1 score.

algorithms (in terms of AUC, F1 Score, and MCC) were used to rank SNPs based on feature importance.

From the results, we observed three cases of gene identification: first, no gene was identified; second, there was

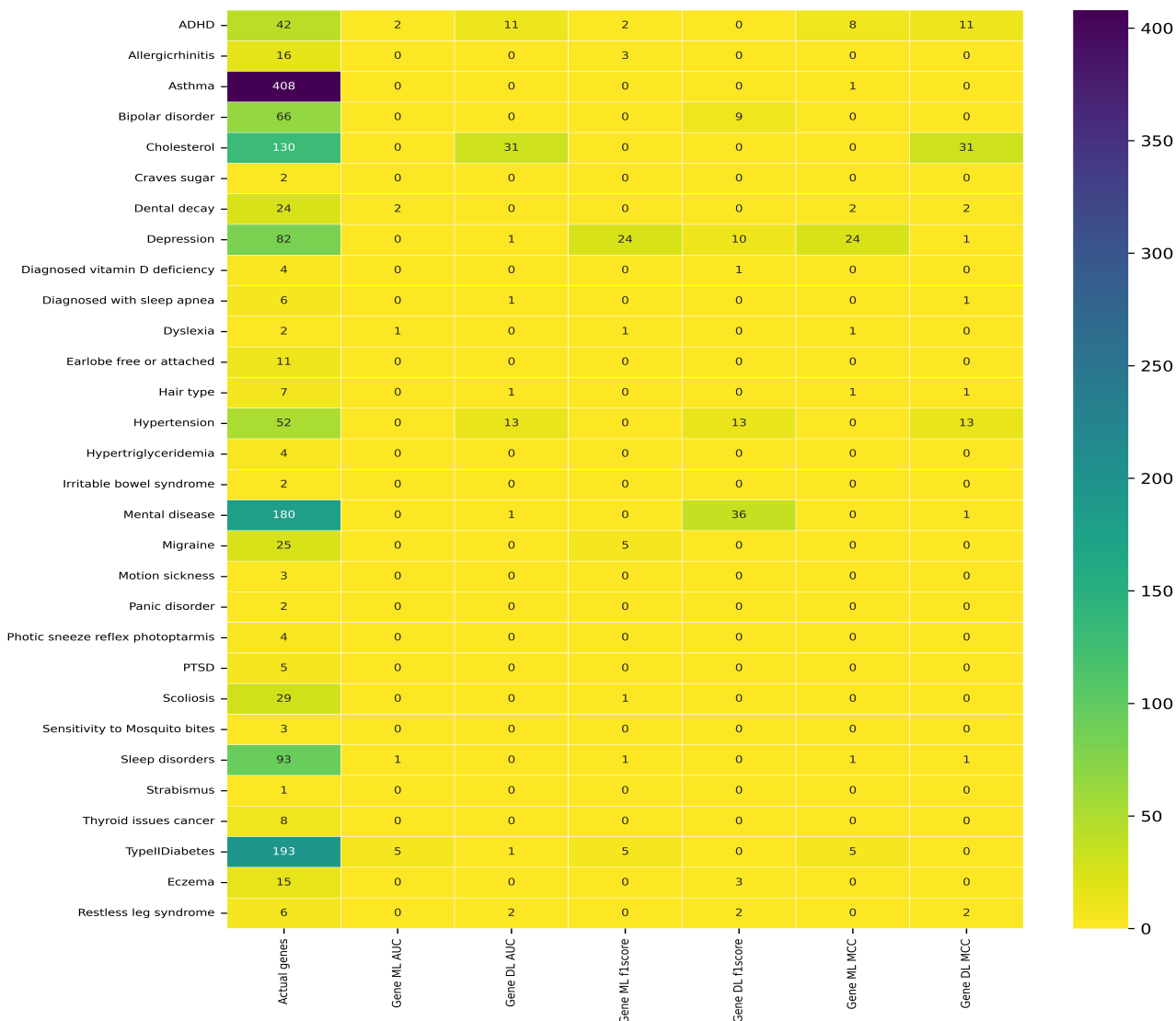


Fig. 4. Heatmap of genes identified by the best-performing ML/DL models according to AUC, F1 score, and MCC. The first column shows the number of SNPs or genes overlapping between the genotype dataset and the GWAS Catalog. ML and DL denote machine learning and deep learning, respectively. Columns 2–7 show the number of SNPs identified by ML and DL models that achieved the best performance for AUC, F1 score, and MCC.

	Machine learning	Deep learning
AUC	0.02	0.06
F1 Score	-0.18	0.1
MCC	-0.08	0.11

Table 4. A table showing the correlation between the best-performing model’s classification score and the number of genes identified.

a high correlation between high classification performance and the number of genes identified; third, genes were identified by either the machine or deep learning algorithm, independent of performance.

For 11 phenotypes, no common gene was identified by either the ML/DL algorithms, even though both achieved high classification performance (colored grey in Table 5). There are four potential reasons why no gene was identified despite a

good performance by a machine or deep learning algorithm: (1) genotype data quality, with low coverage SNPs discarded by the algorithms; (2) linkage disequilibrium can remove highly linked SNPs; (3) the non-linear nature of the machine and deep learning algorithm, leading to combinations of unrelated SNPs being given more weight than causative SNPs [63]; or (4) population structure, as the reported causative genes on the GWAS Catalog may come from different population distributions than the sample population [64].

In the second gene identification scenario, there was a strong correlation between the number of genes identified and the algorithm’s performance. For nine phenotypes (shown in green in Table 5), the machine and deep learning algorithms exhibited robust, generalizable performance, resulting in more causative genes being identified. This aligns with the assumption that optimal algorithms would identify SNPs that yield a better separation boundary between cases and controls. The gene

identification ratio (GIR; Equation 1) for most of these phenotypes was between 0.1 and 0.3.

Gene Identification Ratio =

$$\frac{\text{Number of Genes Identified by Machine/Deep Learning}}{\text{Number of genes from the GWAS Catalog}} \quad (1)$$

In the third gene identification case, the machine or deep learning algorithm identified the causative genes, but this was not linked to performance metrics (as shown in yellow in Table 5). The reason is that ML/DL algorithms use different classification methods. To address this issue, we considered combining the genes identified by both methods and developed an ensemble approach to improve gene identification, as we have done in this study.

We further investigated the gene identification results to identify the reasons for the three cases reported in Table 5.

We applied p-value thresholds to reduce the number of SNPs and used those SNPs for model training. The purpose is to determine the minimum number of SNPs that maximizes classification performance. When SNPs are reduced, the actual number of common SNPs between the data and the GWAS Catalog is reduced. We counted the common SNPs from the best-performing p-value threshold and the GWAS Catalog for each phenotype to further explore this (see Table 6, column (A2)).

After this process, we calculated the gene identification ratio for each phenotype (see Table 6, column (New GIR)), and it changed the results, highlighting that common SNPs have been reduced. The discarded SNPs do not appear in the p-value threshold applied to the GWAS summary statistic file, suggesting that they are less associated with the phenotype under consideration in our dataset.

Table 6 shows the new gene identification ratio for each phenotype. Overall, the mean of the per-phenotype gene identification ratios was 0.84; however, phenotypes with very few GWAS-overlapping genes can disproportionately inflate or deflate this average, so it should be interpreted alongside the individual ratios in Table 6.

We found that individual missingness impacts gene identification performance. We calculated missingness per individual for each phenotype using PLINK. We found a statistically non-significant inverse correlation of -0.15 between the number of genes identified and the missingness per individual, suggesting that higher genotype rates are associated with more common genes identified by machine/deep learning.

Phenotypes	CMA	GMA	CMF	GMF	CMM	GMM	CDA	GDA	CDF	GDF	CDM	GDM	I	A
ADHD	56.6	2	45.4	2	12.2	8	55.6	11	40.6	0	14	11	13	42
Allergic rhinitis	66.2	0	11.4	3	0	0	67.4	0	18.2	0	18.6	0	3	16
Asthma	62.6	0	37.4	0	15.6	1	63.2	0	42.2	0	22.2	0	1	408
Bipolar disorder	73.2	0	88	0	36.2	0	73	0	77.4	9	40.8	0	9	66
Cholesterol	65.4	0	51.8	0	25.6	0	63.8	31	53.6	0	27.4	31	31	130
Craves sugar	82.8	0	92	0	31.8	0	78	0	89.4	0	46.6	0	0	2
Dental decay	66	2	90	0	24.8	2	72	0	78.4	0	35.6	2	2	24
Depression	66	0	37.4	24	22.6	24	62.2	1	43	10	23	1	24	82
Diagnosed vitamin D deficiency	60.8	0	38	0	13.2	0	58.2	0	39.6	1	15	0	1	4
Diagnosed with sleep apnea	67	0	55.8	0	30	0	66.4	1	61.4	0	34	1	1	6
Dyslexia	63.6	1	30	1	19	1	65.6	0	36.8	0	29.4	0	1	2
Earlobe free or attached	63.2	0	43.4	0	29.6	0	64.6	0	46	0	25.4	0	0	11
Hair type	66.4	0	38	0	25.6	1	58.8	1	42.4	0	23.4	1	1	7
Hypertension	79.8	0	91	0	58	0	83.2	13	94	13	64.8	13	13	52
Hypertriglyceridemia	62.4	0	64.6	0	25.4	0	64.8	0	67.8	0	33.2	0	0	4
Irritable bowel syndrome	59.8	0	48.2	0	15.8	0	54.8	0	51.6	0	10.6	0	0	2
Mental disease	60.4	0	49.2	0	20.4	0	60	1	49	36	19.6	1	36	180
Migraine	64.2	0	71.2	5	29	0	56.8	0	61	0	16	0	5	25
Motion sickness	62.6	0	61	0	23.8	0	59.6	0	65.4	0	20.8	0	0	3
Panic disorder	65.6	0	45.2	0	13	0	57.4	0	49.8	0	16	0	0	2
Photoc sneeze reflex (photoptarmic reflex)	60	0	61	0	21	0	65.8	0	64.4	0	33	0	0	4
PTSD	74	0	84.4	0	12.8	0	64.6	0	72	0	27.8	0	0	5
Scoliosis	69.8	0	57.8	1	32.2	0	69.6	0	67.2	0	41.2	0	1	29
Sensitivity to Mosquito bites	61	0	46.4	0	12.4	0	68.4	0	57.6	0	35.8	0	0	3
Sleep disorders	68.4	1	36.8	1	25.2	1	66.8	0	34.4	0	23.4	1	1	93
Strabismus	67.8	0	38.8	0	26.2	0	71	0	43	0	32.6	0	0	1
Thyroid issues cancer	76	0	63.8	0	35.4	0	71.4	0	65.2	0	46.6	0	0	8
TypeIIDiabetes	69.6	5	36.2	5	26.8	5	78.6	1	48.6	0	41.8	0	5	193
Eczema	83.2	0	71.2	0	52.2	0	64.8	0	60.2	3	32.8	0	3	15
Restless leg syndrome	66	0	46	0	30.4	0	54.8	2	42.2	2	6.6	2	2	6

Table 5. A table showing the AUC, MCC, and F1 Score and the number of genes identified by each model. In this table, labels for the first 12 columns are shown in this format (XYZ). X can be [C, G], where C = the classification performance and G = the number of genes identified. Y can be [M, DJ], where M means machine learning and D means deep learning. Z can be [A, F, M], where A = AUC, F = F1 score, and M = MCC. I means the total number of genes identified by the machine and deep learning algorithm combined. The last column A shows the number of genes associated with the phenotype. There are three color codes, green, yellow, and gray, which are explained in the text.

Phenotypes	A	I	GIR	A2	New GIR
ADHD	42	13	0.31	14	0.93
Allergic rhinitis	16	3	0.19	3	1
Asthma	408	1	0.0	1	1
Bipolar disorder	66	9	0.14	13	0.69
Cholesterol	130	31	0.24	38	0.81
Craves sugar	2	0	0.0	0	-
Dental decay	24	2	0.08	2	1
Depression	82	24	0.29	24	1
Diagnosed vitamin D deficiency	4	1	0.25	1	1
Diagnosed with sleep apnea	6	1	0.17	2	0.5
Dyslexia	2	1	0.5	1	1
Earlobe free or attached	11	0	0.0	0	-
Hair type	7	1	0.14	0	-
Hypertension	52	13	0.25	13	1
Hypertriglyceridemia	4	0	0.0	0	-
Irritable bowel syndrome	2	0	0.0	1	0
Mental disease	180	36	0.2	45	0.8
Migraine	25	5	0.2	5	1
Motion sickness	3	0	0.0	0	-
Panic disorder	2	0	0.0	0	-
Photoc sneeze reflex (photoptarmic reflex)	4	0	0.0	1	0
PTSD	5	0	0.0	0	-
Scoliosis	29	1	0.03	1	1
Sensitivity to Mosquito bites	3	0	0.0	0	-
Sleep disorders	93	1	0.01	1	1
Strabismus	1	0	0.0	0	-
Thyroid issues cancer	8	0	0.0	0	-
TypeIIDiabetes	193	5	0.03	10	0.5
Eczema	15	3	0.2	3	1
Restless leg syndrome	6	2	0.33	2	1

Table 6. A table showing the new gene identification ratio associated with each phenotype. In this table, the first column shows the phenotype, the second column (A) shows the number of common genes between our genotype data and the one downloaded from the GWAS Catalog, the third column (I) shows the number of common genes identified by machine/deep learning and the one listed in the second column (A), and the fourth column (GIR) shows the gene identification ratio for each phenotype as specified in Equation 1 and calculated by dividing the third column by the second column (I/A). The fifth column (A2) shows the number of common genes between the one downloaded from the GWAS Catalog and identified by machine/deep learning after p-values thresholding, and the last column shows the final gene identification ratio calculated by dividing ($I/A2$). "-" indicates that the values in A2 are 0, resulting in division by zero.

Table 7 shows the correlation between the New GIR (see Table 6, column **New GIR**) and the performance of machine/deep learning algorithms in terms of AUC, F1 Score, and MCC. It suggests that a deep learning algorithm optimized for the F1 Score achieves a higher identification ratio than models optimized for other evaluation metrics.

	Machine learning	Deep learning
AUC	0.06	0.34
F1 Score	0.23	0.40
MCC	0.24	0.35

Table 7. A table showing the correlation between the New GIR and the performance of the machine/deep learning algorithms.

Supplementary material (Section 3) lists the common genes between the ones identified by the machine and deep learning algorithms and those listed on the GWAS Catalog for each phenotype. The phenotypes, the number of associated genes from the GWAS Catalog for each phenotype, and the number of common genes and SNPs identified by ML/DL and from the GWAS Catalog for each phenotype are available on GitHub (Final_Results.pdf).

We identified the common SNPs and genes among all phenotypes. Identifying the shared genes between phenotypes is of great importance. It helps identify shared gene influences across multiple phenotypes and genes associated with more than one phenotype.

We have presented two heatmaps illustrating the overlap of genetic factors among phenotypes: one depicting the number of common SNPs (Figure 5), and the other showing the number of common genes (Figure 6). The number of common genes (Figure 6) between two phenotypes is greater than the number of common SNPs (Figure 5) because the actual associated SNPs can be different, but the genes in which these SNPs are present can be the same.

Figure 5 shows one common SNP between Depression, Mental Disease and ADHD, which is also a neuro-developmental disorder. There is also one common SNP between Depression, Mental Disease, and Bipolar Disorder, a mental health condition. There is a common SNP between Depression and Mental Disease. These findings suggest that machine-learning and deep-learning algorithms can identify risk variants for some phenotypes and even common risk variants across diseases.

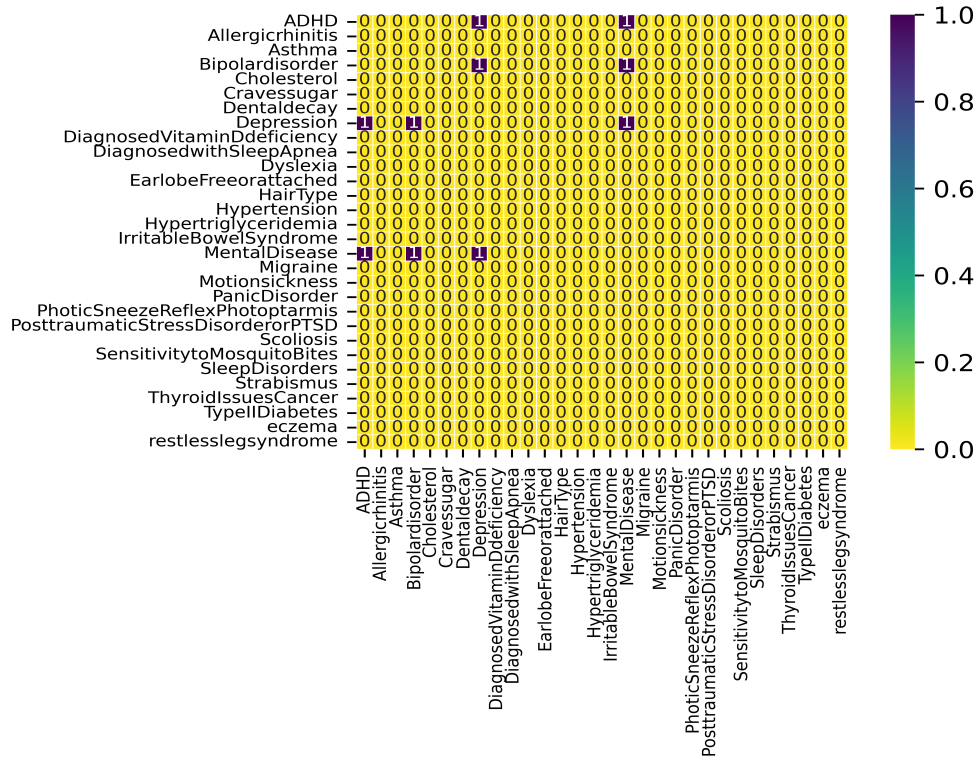


Fig. 5. A heatmap showing the number of common SNPs between phenotypes.

Figure 6 shows one common gene between hypertension and Allergic Rhinitis, Bipolar Disorder, Cholesterol, Depression, and Vitamin D Deficiency.

Conclusion

We have proposed a pipeline to identify genes associated with phenotypes using ML and DL algorithms on openSNP data. The identified genes were compared with the existing associated genes from the GWAS Catalog. The mean of the per-phenotype gene identification ratios was 0.84, though this average is sensitive to phenotypes with very few overlapping genes and should be interpreted alongside the individual ratios. The classification performance of the best-performing models was used to assess the reliability of the identified genes.

In the ML/DL approach, combining two or more SNPs, which may be biologically irrelevant, can encode more information than a single SNP selected by GWAS, thereby reducing the gene identification ratio. The quantity and quality of genotype data can affect the genes identified by machine learning, and results can be improved by including all SNPs and genes in the dataset.

We observed that p-value thresholds affect gene identification performance. The optimal number of SNPs for classification performance is limited. In that case, the SNPs associated with the phenotypes downloaded from the GWAS Catalog may not even appear in the final results. SNPs from the GWAS Catalog for a particular phenotype are collected across multiple studies and data sources, and it is likely that none of these SNPs are significant for the sample dataset. Although other models perform well when a large number of SNPs are used for training, this undermines the study’s rationale, which suggests choosing

the model that achieves high performance with a minimal number of SNPs.

Our main focus was to identify genes associated with specific phenotypes using machine learning and compare them with existing genes associated with the same phenotype. It is possible that the identified genes differ, but rather than using machine learning for identification, we can use the proposed pipeline as a pre-processing step for GWAS, allowing exploration of various genomic regions that can be further scanned to identify potential association candidates.

Calculating feature weights is time-consuming during training deep learning models, so we recommend first identifying the best-performing algorithms and retraining those models to obtain the weights.

The code for this study is available on GitHub <https://github.com/MuhammadMuneeb007/Identifying-genes-associated-with-30-phenotypes-using-machine-deep-learning->.

Key Points

- This study proposes a pipeline to identify genes associated with phenotypes using machine-learning and deep-learning algorithms.
- The best-performing models, optimized for evaluation metrics such as AUC, MCC, and F1-Score, can be combined to identify important features or SNPs that assist in gene identification.
- Genotype data quality, the population under study, the number of variants, missingness per person, and the p-value threshold of the best-performing models affect the gene identification ratio.

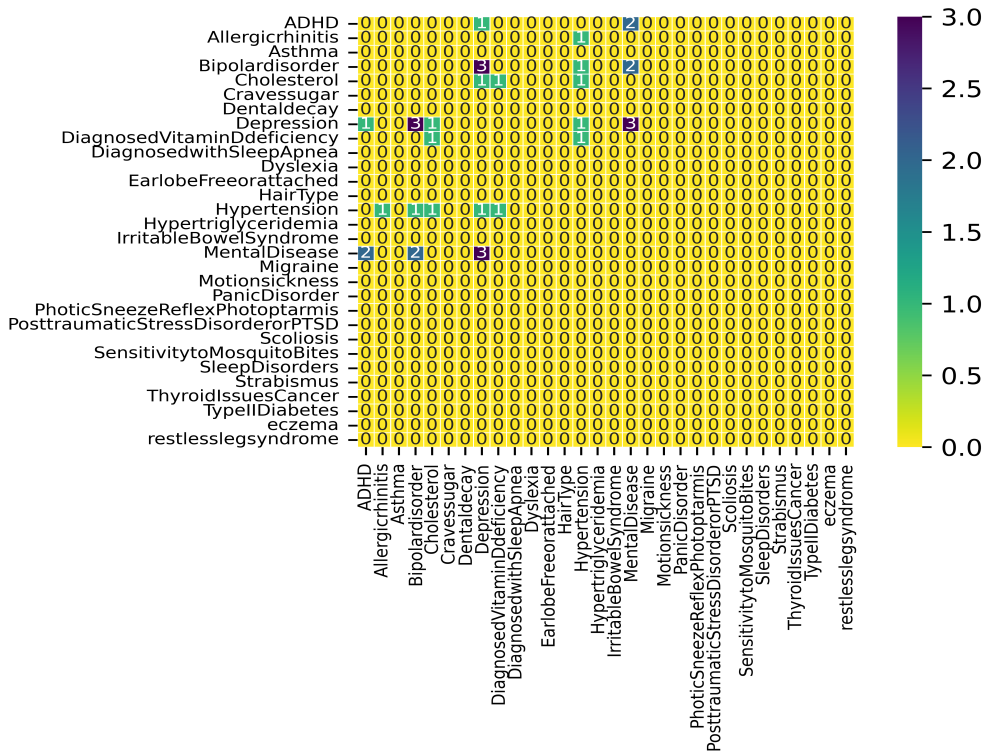


Fig. 6. A heatmap showing the number of common genes between phenotypes.

- The mean of the per-phenotype gene identification ratios was 0.84, though individual ratios vary widely across phenotypes.

Competing interests

The authors declare that they have no competing interests.

Author contributions statement

M.M. wrote the first draft of the manuscript. M.M. and Y.M. analyzed the results. D.A., M.M., and Y.M. reviewed and edited the manuscript. M.M. and D.A. contributed to the manuscript's methodology.

Data availability

The dataset used in this study is available from openSNP (<http://opensnp.org/>), and the code is available on GitHub (<https://github.com/MuhammadMuneeb007/Identifying-genes-associated-with-30-phenotypes-using-machine-deep-learning->).

Acknowledgments

Not applicable.

References

1. Aline Jelenkovic, Reijo Sund, Yoshie Yokoyama, Antti Latvala, Masumi Sugawara, Mami Tanaka, Satoko Matsumoto, Duarte L. Freitas, José Antonio Maia, Ariel Knafo-Noam, David Mankuta, Lior Abramson, Fuling Ji, Feng Ning, Zengchang Pang, Esther Rebato, Kimberly J. Saudino, Tessa L. Cutler, John L. Hopper, Vilhelmina Ullemar, Catarina Almqvist, Patrik K. E. Magnusson, Wendy Cozen, Amie E. Hwang, Thomas M. Mack, Tracy L. Nelson, Keith E. Whitfield, Joohon Sung, Jina Kim, Jooyeon Lee, Sooji Lee, Clare H. Llewellyn, Abigail Fisher, Emanuela Medda, Lorenza Nisticò, Virgilia Toccaceli, Laura A. Baker, Catherine Tuvblad, Robin P. Corley, Brooke M. Huibregtse, Catherine A. Derom, Robert F. Vlietinck, Ruth J. F. Loos, S. Alexandra Burt, Kelly L. Klump, Judy L. Silberg, Hermine H. Maes, Robert F. Krueger, Matt McGue, Shandell Pahlen, Margaret Gatz, David A. Butler, Jennifer R. Harris, Ingunn Brandt, Thomas S. Nilsen, K. Paige Harden, Elliot M. Tucker-Drob, Carol E. Franz, William S. Kremen, Michael J. Lyons, Paul Lichtenstein, Meike Bartels, Catharina E. M. van Beijsterveldt, Gonneke Willemsen, Sevgi Y. Öncel, Fazil Aliev, Hoe-Uk Jeong, Yoon-Mi Hur, Eric Turkheimer, Dorret I. Boomsma, Thorkild I. A. Sørensen, Jaakko Kaprio, and Karri Silventoinen. Genetic and environmental influences on human height from infancy through adulthood at different levels of parental education. *Scientific Reports*, 10(1), May 2020.
2. Matt McGue and Thomas J. Bouchard. GENETIC AND ENVIRONMENTAL INFLUENCES ON HUMAN BEHAVIORAL DIFFERENCES. *Annual Review of Neuroscience*, 21(1):1–24, March 1998.
3. S R Jaffee and T S Price. Gene–environment correlations: a review of the evidence and implications for prevention of mental illness. *Molecular Psychiatry*, 12(5):432–442, jan 2007.
4. Gordon H. Williams, Naomi D.L. Fisher, Steve C. Hunt, Xavier Jeunemaitre, Paul N. Hopkins, and Norman K. Hollenberg. Effects of gender and genotype on the phenotypic expression of nonmodulating essential hypertension. *Kidney International*, 57(4):1404–1407, apr 2000.
5. David J. Hunter. Gene–environment interactions in human diseases. *Nature Reviews Genetics*, 6(4):287–298, April 2005.
6. Stylianos E. Antonarakis. History of the methodology of disease gene identification. *American Journal of Medical Genetics Part A*, 185(11):3266–3275, June 2021.
7. James W. Fickett. The gene identification problem: An overview for developers. *Computers & Chemistry*, 20(1):103–118, March 1996.
8. Ahmad M. Alqudah, Ahmed Sallam, P. Stephen Baenziger, and Andreas Börner. GWAS: Fast-forwarding gene identification and characterization in temperate cereals: lessons from barley – a review. *Journal of Advanced Research*, 22:119–135, March 2020.
9. Aedan G K Roberts, Daniel R Catchpoole, and Paul J Kennedy. Identification of differentially distributed gene expression and distinct sets of cancer-related genes identified by changes in mean and variability. *NAR Genomics and Bioinformatics*, 4(1), January 2022.
10. Elisa Cirillo, Laurence D. Parnell, and Chris T. Evelo. A review of pathway-based analysis tools that visualize genetic variants. *Frontiers in Genetics*, 8, November 2017.
11. Guanming Wu, Xin Feng, and Lincoln Stein. A human functional protein interaction network and its application to cancer data analysis. *Genome Biology*, 11(5):R53, 2010.
12. Binglan Li and Marylyn D. Ritchie. From GWAS to gene: Transcriptome-wide association studies and other methods to functionally understand GWAS discoveries. *Frontiers in Genetics*, 12, September 2021.
13. Nivedhitha Mahendran, P. M. Durai Raj Vincent, Kathiravan Srinivasan, and Chuan-Yu Chang. Machine learning based computational gene selection models: A survey, performance evaluation, open issues, and future research directions. *Frontiers in Genetics*, 11, December 2020.
14. Nicholas Pudjihartono, Tayaza Fadason, Andreas W. Kempa-Liehr, and Justin M. O'Sullivan. A review of feature selection methods for machine learning-based disease risk prediction. *Frontiers in Bioinformatics*, 2, June 2022.
15. Anthony M. Musolf, Emily R. Holzinger, James D. Malley, and Joan E. Bailey-Wilson. What makes a good prediction? feature importance and beginning to open the black box of machine learning in genetics. *Human Genetics*, 141(9):1515–1528, December 2021.
16. Luis G Leal, Alessia David, Marjo-Riita Jarvelin, Sylvain Sebert, Minna Männikkö, Ville Karhunen, Eleanor Seaby, Clive Hoggart, and Michael J E Sternberg. Identification of disease-associated loci using machine learning for genotype and network data integration. *Bioinformatics*, 35(24):5182–5190, May 2019.
17. Ignacio San Segundo-Val and Catalina S. Sanz-Lozano. Introduction to the gene expression analysis. In *Methods in Molecular Biology*, pages 29–43. Springer New York, 2016.
18. Saroj Ghadle, Rakesh Tripathi, Sanjay Kumar, and Vandana Munde. Study on analysis of gene expression dataset and identification of differentially expressed genes. In *Intelligent Computing and Networking*, pages 253–259. Springer Singapore, October 2020.
19. Pyingkodi Maran, Shanthi S., Thenmozhi K., Hemalatha D., and Nanthini K. A novel deep learning method for identification of cancer genes from gene expression dataset. In *Machine Learning and Deep Learning in Real-Time*

- Applications*, pages 129–144. IGI Global, 2020.
20. Arfa Anjum, Seema Jaggi, Eldho Varghese, Shwetank Lall, Arpan Bhowmik, and Anil Rai. Identification of differentially expressed genes in rna-seq data of arabidopsis thaliana: A compound distribution approach. *Journal of Computational Biology*, 23(4):239–247, April 2016.
 21. Houxi Xu, Yuzhu Ma, Jinzhi Zhang, Jialin Gu, Xinyue Jing, Shengfeng Lu, Shuping Fu, and Jiege Huo. Identification and verification of core genes in colorectal cancer. *BioMed Research International*, 2020:1–13, May 2020.
 22. Shemim Begum, Ram Sarkar, Debasis Chakraborty, Sagnik Sen, and Ujjwal Maulik. Application of active learning in DNA microarray data for cancerous gene identification. *Expert Systems with Applications*, 177:114914, September 2021.
 23. Wenzong Lu and Zhe Ding. Identification of key genes in prostate cancer gene expression profile by bioinformatics. *Andrologia*, 51(1):e13169, October 2018.
 24. S. P. B. M Senadheera and A. R. Weerasinghe. Hub genes identification in brain cancer with gene expression data. In *2020 20th International Conference on Advances in ICT for Emerging Regions (ICTer)*. IEEE, November 2020.
 25. Yang Liu, Duolin Wang, Fei He, Juexin Wang, Trupti Joshi, and Dong Xu. Phenotype prediction and genome-wide association study using deep convolutional neural network of soybean. *Frontiers in Genetics*, 10, November 2019.
 26. Medi Kori and Esra Gov. Bioinformatics prediction and machine learning on gene expression data identifies novel gene candidates in gastric cancer. *Genes*, 13(12):2233, November 2022.
 27. Sahra Uygun, Cheng Peng, Melissa D. Lehti-Shiu, Robert L. Last, and Shin-Han Shiu. Utility and limitations of using gene expression data to identify functional associations. *PLOS Computational Biology*, 12(12):e1005244, December 2016.
 28. Emil Uffelmann, Qin Qin Huang, Nchangwi Syntia Munung, Jantina de Vries, Yukinori Okada, Alicia R. Martin, Hilary C. Martin, Tuuli Lappalainen, and Danielle Posthuma. Genome-wide association studies. *Nature Reviews Methods Primers*, 1(1), August 2021.
 29. Eddie Cano-Gamez and Gosia Trynka. From GWAS to function: Using functional genomics to identify the mechanisms underlying complex diseases. *Frontiers in Genetics*, 11, May 2020.
 30. Andries T. Marees, Hilde de Kluiver, Sven Stringer, Florence Vorspan, Emmanuel Curis, Cynthia Marie-Claire, and Eske M. Derks. A tutorial on conducting genome-wide association studies: Quality control and statistical analysis. *International Journal of Methods in Psychiatric Research*, 27(2):e1608, February 2018.
 31. Brenda Udosen, Opeyemi Soremekun, Abram Kamiza, Tafadzwa Machipisa, Cisse Cheickna, Olaposi Omotuyi, Mahmoud Soliman, Mamadou Wélé, Oyekanmi Nashiru, Tinashe Chikowore, and Segun Fatumo. Meta-analysis and multivariate GWAS analyses in 77, 850 individuals of african ancestry identify novel variants associated with blood pressure traits. *International Journal of Molecular Sciences*, 24(3):2164, January 2023.
 32. Demis A. Kia, David Zhang, Sebastian Guelfi, Claudia Manzoni, Leon Hubbard, Regina H. Reynolds, Juan Botía, Mina Ryten, Raffaele Ferrari, Patrick A. Lewis, Nigel Williams, Daniah Trabzuni, John Hardy, Nicholas W. Wood, Alastair J. Noyce, Rauan Kaiyrzhanov, Ben Middlehurst, Demis A. Kia, Manuela Tan, Henry Houlden, Huw R. Morris, Helene Plun-Favreau, Peter Holmans, John Hardy, Daniah Trabzuni, Jose Bras, John Quinn PhD, Kin Y. Mok, Kerri J. Kinghorn, Kimberley Billingsley, Nicholas W. Wood, Patrick Lewis, Sebastian Schreglmann, Rita Guerreiro, Ruth Lovering, Lea R'Bibo, Claudia Manzoni, Mie Rizig, Mina Ryten, Sebastian Guelfi, Valentina Escott-Price, Viorica Chelban, Thomas Foltynie, Nigel Williams, Alexis Brice, Fabrice Danjou, Suzanne Lesage, Jean-Christophe Corvol, Maria Martinez, Claudia Schulte, Kathrin Brockmann, Javier Simón-Sánchez, Peter Heutink, Patrizia Rizzo, Manu Sharma, Thomas Gasser, Aude Nicolas, Mark R. Cookson, Sara Bandres-Ciga, Cornelis Blauwendraat, David W. Craig, Faraz Faghri, J. Raphael Gibbs, Dena G. Hernandez, Kendall Van Keuren-Jensen, Joshua M. Shulman, Hampton L. Leonard, Mike A. Nalls, Laurie Robak, Steven Lubbe, Steven Finkbeiner, Niccolo E. Mencacci, Codrin Lungu, Andrew B Singleton, Sonja W. Scholz, Xylena Reed, Roy N. Alcalay, Ziv Gan-Or, Guy A. Rouleau, Lynne Krohn, Jacobus J. van Hilten, Johan Marinus, Astrid D. Adames-Gómez, Miquel Aguilar, Ignacio Alvarez, Victoria Alvarez, Francisco Javier Barrero, Jesús A. Bergareche Yarza, Inmaculada Bernal-Bernal, Marta Blazquez, Marta Bonilla-Toribio, Juan A. Botía, María T. Bongiorno, Dolores Buiza-Rueda, Ana Càmara, Fátima Carrillo, Mario Carrión-Claro, Debora Cerdan, Jordi Clarimón, Yaroslau Compta, Monica Diez-Fairen, Oriol Dols-Icardo, Jacinto Duarte, Raquel Duran, Francisco Escamilla-Sevilla, Mario Ezquerro, Cici Feliz, Manel Fernández, Rubén Fernández-Santiago, Ciara Garcia, Pedro García-Ruiz, Pilar Gómez-Garre, Maria J. Gomez Heredia, Isabel Gonzalez-Aramburu, Ana G. Pagola, Janet Hoenicka, Jon Infante, Adriano Jimenez-Escrig, Jaime Kulisevsky, Miguel A. Labrador-Espinosa, Jose Luis Lopez-Sendon, Adolfo López de Munain Arregui, Daniel Macias, Irene Martínez Torres, Juan Marín, Maria Jose Marti, Juan Carlos Martínez-Castrillo, Carlota Mèndez del Barrio, Manuel Menéndez González, Marina Mata Adolfo Mínguez, Pablo Mir, Elisabet Mondragon Rezola, Esteban Muñoz, Javier Pagonabarraga, Pau Pastor, Francisco Perez Errazquin, Teresa Perinán-Tocino, Javier Ruiz-Martínez, Clara Ruz, Antonio Sanchez Rodriguez, María Sierra, Esther Suarez-Sanmartin, Cesar Tabernero, Juan Pablo Tartari, Cristina Tejera-Parrado, Eduard Tolosa, Francesc Valdeoriola, Laura Vargas-González, Lydia Vela, Francisco Vives, Alexander Zimprich, Lasse Pihlstrom, Mathias Toft, Sulev Koks, Pille Taba, Sharon Hassin-Baer, Michael Weale, Adaikalavan Ramasamy, Colin Smith, Manuel Sebastian Guelfi, Karishma D'sa, Paola Forabosco, and Juan A. Botía and. Identification of candidate parkinson disease genes by integrating genome-wide association study, expression, and epigenetic data sets. *JAMA Neurology*, 78(4):464, April 2021.
 33. Shea J. Andrews, Alan E. Renton, Brian Fulton-Howard, Anna Podlesny-Drabiniok, Edoardo Marcora, and Alison M. Goate. The complex genetic architecture of alzheimer's disease: novel insights and future directions. *eBioMedicine*, 90:104511, April 2023.
 34. Mitchell Gill, Robyn Anderson, Haifei Hu, Mohammed Bennamoun, Jakob Petereit, Babu Valliyodan, Henry T. Nguyen, Jacqueline Batley, Philipp E. Bayer, and David Edwards. Machine learning models outperform deep learning models, provide interpretation and facilitate feature selection for soybean trait prediction. *BMC Plant*

- Biology*, 22(1), April 2022.
35. Bo Li, Nanxi Zhang, You-Gan Wang, Andrew W. George, Antonio Reverter, and Yutao Li. Genomic prediction of breeding values using a subset of SNPs identified by three machine learning methods. *Frontiers in Genetics*, 9, July 2018.
 36. Joverlyn Gaudillo, Jae Joseph Russell Rodriguez, Allen Nazareno, Lei Rigi Baltazar, Julianne Vilela, Rommel Bulalacao, Mario Domingo, and Jason Albia. Machine learning approach to single nucleotide polymorphism-based asthma prediction. *PLOS ONE*, 14(12):e0225574, December 2019.
 37. Ashraf Abou Tabl, Abedalrhman Alkhateeb, Waguih ElMaraghy, Luis Rueda, and Alioune Ngom. A machine learning approach for identifying gene biomarkers guiding the treatment of breast cancer. *Frontiers in Genetics*, 10, March 2019.
 38. Xinlei Mi, Baiming Zou, Fei Zou, and Jianhua Hu. Permutation-based identification of important biomarkers for complex diseases via machine learning models. *Nature Communications*, 12(1), May 2021.
 39. Yasukuni Mori, Hajime Yokota, Isamu Hoshino, Yosuke Iwatate, Kohei Wakamatsu, Takashi Uno, and Hiroki Suyari. Deep learning-based gene selection in comprehensive gene analysis in pancreatic cancer. *Scientific Reports*, 11(1), August 2021.
 40. Rahul Gomes, Nijhum Paul, Nichol He, Aaron Francis Huber, and Rick J. Jansen. Application of feature selection and deep learning for cancer prediction using DNA methylation markers. *Genes*, 13(9):1557, August 2022.
 41. Abbas Saad Alatrany, Wasiq Khan, Abir Hussain, and Dhiya Al-Jumeily and. Wide and deep learning based approaches for classification of alzheimer's disease using genome-wide association studies. *PLOS ONE*, 18(5):e0283712, May 2023.
 42. Elizabeth H. Mahood, Lars H. Kruse, and Gaurav D. Moghe. Machine learning: A powerful tool for gene function prediction in plants. *Applications in Plant Sciences*, 8(7), July 2020.
 43. Brett A McKinney, David M Reif, Marylyn D Ritchie, and Jason H Moore. Machine learning for detecting gene-gene interactions. *Applied Bioinformatics*, 5(2):77–88, 2006.
 44. Mostafa Abbas and Yasser EL-Manzalawy. Machine learning based refined differential gene expression analysis of pediatric sepsis. *BMC Medical Genomics*, 13(1), August 2020.
 45. Bastian Greshake, Philipp E. Bayer, Helge Rausch, and Julia Reda. openSNP—a crowdsourced web resource for personal genomics. *PLoS ONE*, 9(3):e89204, March 2014.
 46. Mark I. McCarthy, Gonçalo R. Abecasis, Lon R. Cardon, David B. Goldstein, Julian Little, John P. A. Ioannidis, and Joel N. Hirschhorn. Genome-wide association studies for complex traits: consensus, uncertainty and challenges. *Nature Reviews Genetics*, 9(5):356–369, May 2008.
 47. David G Clayton, Neil M Walker, Deborah J Smyth, Rebecca Pask, Jason D Cooper, Lisa M Maier, Luc J Smink, Alex C Lam, Nigel R Ovington, Helen E Stevens, Sarah Nutland, Joanna M M Howson, Malek Faham, Martin Moorhead, Hywel B Jones, Matthew Falkowski, Paul Hardenbol, Thomas D Willis, and John A Todd. Population structure, differential bias and genomic control in a large-scale, case-control association study. *Nature Genetics*, 37(11):1243–1246, October 2005.
 48. Lizhi Liao, Heng Li, Weiyi Shang, and Lei Ma. An empirical study of the impact of hyperparameter tuning and model optimization on the performance properties of deep neural networks. *ACM Transactions on Software Engineering and Methodology*, 31(3):1–40, April 2022.
 49. Steven A. Hicks, Inga Strümke, Vajira Thambawita, Malek Hammou, Michael A. Riegler, Pål Halvorsen, and Sravanthi Parasa. On evaluation metrics for medical applications of artificial intelligence. *Scientific Reports*, 12(1), April 2022.
 50. F. Pedregosa, G. Varoquaux, A. Gramfort, V. Michel, B. Thirion, O. Grisel, M. Blondel, P. Prettenhofer, R. Weiss, V. Dubourg, J. Vanderplas, A. Passos, D. Cournapeau, M. Brucher, M. Perrot, and E. Duchesnay. Scikit-learn: Machine learning in Python. *Journal of Machine Learning Research*, 12:2825–2830, 2011.
 51. Bahzad Jijo and Adnan Mohsin Abdulazeez. Classification based on decision tree algorithm for machine learning. *Journal of Applied Science and Technology Trends*, 2:20–28, 01 2021.
 52. Tianqi Chen and Carlos Guestrin. XGBoost: A scalable tree boosting system. In *Proceedings of the 22nd ACM SIGKDD International Conference on Knowledge Discovery and Data Mining*, KDD '16, pages 785–794, New York, NY, USA, 2016. ACM.
 53. Nello Cristianini and Elisa Ricci. Support vector machines. In *Encyclopedia of Algorithms*, pages 928–932. Springer US, 2008.
 54. Mirka Saarela and Susanne Jauhiainen. Comparison of feature importance measures as explanations for classification models. *SN Applied Sciences*, 3(2), February 2021.
 55. Rung-Ching Chen, Christine Dewi, Su-Wen Huang, and Rezy Eko Caraka. Selecting critical features for data classification based on machine learning methods. *Journal of Big Data*, 7(1), July 2020.
 56. Warren S McCulloch and Walter Pitts. A logical calculus of the ideas immanent in nervous activity. *The bulletin of mathematical biophysics*, 5(4):115–133, 1943.
 57. Rahul Dey and Fathi M. Salem. Gate-variants of gated recurrent unit (gru) neural networks. In *2017 IEEE 60th International Midwest Symposium on Circuits and Systems (MWSCAS)*, pages 1597–1600, 2017.
 58. Sepp Hochreiter and Jürgen Schmidhuber. Long short-term memory. *Neural Computation*, 9(8):1735–1780, November 1997.
 59. M. Schuster and K.K. Paliwal. Bidirectional recurrent neural networks. *IEEE Transactions on Signal Processing*, 45(11):2673–2681, 1997.
 60. Joaquín Figueroa Barraza, Enrique López Droguett, and Marcelo Ramos Martins. Towards interpretable deep learning: A feature selection framework for prognostics and health management using deep neural networks. *Sensors*, 21(17):5888, September 2021.
 61. Jie Cai, Jiawei Luo, Shulin Wang, and Sheng Yang. Feature selection in machine learning: A new perspective. *Neurocomputing*, 300:70–79, 2018.
 62. Maksymilian Wojtas and Ke Chen. Feature importance ranking for deep learning. In H. Larochelle, M. Ranzato, R. Hadsell, M.F. Balcan, and H. Lin, editors, *Advances in Neural Information Processing Systems*, volume 33, pages 5105–5114. Curran Associates, Inc., 2020.
 63. Sayan Roy and Debanjan Rana. Machine learning in nonlinear dynamical systems. *Resonance*, 26(7):953–970, July 2021.

64. Luis B Barreiro, Guillaume Laval, Hélène Quach, Etienne Patin, and Lluís Quintana-Murci. Natural selection has driven population differentiation in modern humans. *Nature Genetics*, 40(3):340–345, February 2008.

PAPER

Identifying genes associated with phenotypes using machine and deep learning

Muhammad Muneeb,^{1,2} David B. Ascher^{1,2,*} and YooChan Myung^{1,2}

¹School of Chemistry and Molecular Biology, The University of Queensland, Queen Street, 4067, Queensland, Australia and

²Computational Biology and Clinical Informatics, Baker Heart and Diabetes Institute, Commercial Road, 3004, Victoria, Australia

*Corresponding authors: David B. Ascher, Email: d.ascher@uq.edu.au

FOR PUBLISHER ONLY Received on Date Month Year; revised on Date Month Year; accepted on Date Month Year

Abstract

Supplementary Material 1.

Supplementary Material 1

This section describes the dataset, data processing steps, phenotypic value cleaning, and genotype data transformation.

Dataset pre-processing

There were 6,401 genotype files and 668 phenotypes in the openSNP dataset [1], and the phenotype data are available on GitHub (Analysis1.pdf). Only binary phenotypes were considered; phenotypes with missing values were discarded, and each value for each phenotype was assigned to one of three values: Case, Control, or Unknown.

Phenotype values transformation

Participants' phenotypic responses varied, necessitating the cleansing of phenotype data. For example, many terms are used for right-handedness: "right-handed", "right", "Right", and "R". To create cases and controls for each phenotype, we aggregated these occurrences into a single phenotypic value. Other phenotypic value ambiguities are shown on GitHub (AmbiguousPhenotypes.pdf) with examples.

The `preTransform` file, which contains the phenotypic information, the number of values for each phenotype, and its unique values, must be created first. `PreTransform.csv` is available on GitHub and aids in identifying ambiguities in the phenotypic file. The next phase was to create the `postTransform` file, which converts each phenotype's values from multiple values to one of the following for binary classification.

- Cases: Yes (Presence of a particular phenotype value).
- Controls: No (Absence of a particular phenotype value).
- U: Unsure, means we are unsure whether people who selected this phenotype fall in Class1 or Class2.
- x: means this phenotype value is removed from further analysis.

The final `postTransformed` is available on this GitHub (`postTransformed.csv`).

Extract samples for each phenotype

Convert the values in the `preTransform` file to the `postTransform` file, count controls and cases for each phenotype, and finally extract the individuals' genetic files. On GitHub (Analysis2.pdf), you can find the phenotypic name, the number of samples from classes 1 and 2, the total number of samples for each phenotype, and the actual class name. For further analysis, we considered 100 phenotypes.

Genetic file format conversion

The genetic data came in a variety of formats. Thus, we transformed each AncestryDNA file into the 23andMe format before converting it to the PLINK format (bed, bim, fam) [2].

Supplementary Material 2

This section explains the classification results from the machine learning and deep learning models.

Tables 1, 2, and 3 show the best machine learning model, which yielded the best performance in terms of AUC, F1 Score, and MCC. Tables 4, 5, and 6 show the best deep learning model, which yielded the best performance in terms of AUC, F1 Score, and MCC.

Phenotype	AUC	SD	Machine learning algorithm index	Number of SNPs
ADHD	56.6	4.98	Xgboost, Booster: gblinear - Loss function: binary:hinge	5000
Allergicrhinitis	66.2	26.18	Xgboost, Booster: gblinear - Loss function: binary:hinge	200
Asthma	62.6	7.77	Xgboost, Booster: gblinear - Loss function: binary:hinge	1000
Bipolar disorder	73.2	30.36	Xgboost, Booster: gbtree - Loss function: binary:logitraw	500
Cholesterol	65.4	8.93	Xgboost, Booster: gbtree - Loss function: binary:hinge	5000
Craves sugar	82.8	18.34	Xgboost, Booster: gblinear - Loss function: binary:logistic	500
Dental decay	66.0	8.94	PassiveAggressiveClassifier	500
Depression	66.0	20.64	Xgboost, Booster: gblinear - Loss function: binary:hinge	10000
Diagnosed vitamin D deficiency	60.8	14.52	Xgboost, Booster: gblinear - Loss function: binary:hinge	200
Diagnosed with sleep apnea	67.0	8.37	Xgboost, Booster: gblinear - Loss function: binary:logistic	100
Dyslexia	63.6	3.29	SGDClassifier	10000
Earlobe free or attached	63.2	12.56	RidgeClassifier	50
Hair type	66.4	11.06	Xgboost, Booster: gblinear - Loss function: binary:logistic	1000
Hypertension	79.8	21.82	DecisionTreeClassifier	500
Hypertriglyceridemia	62.4	17.5	PassiveAggressiveClassifier	50
Irritable bowel syndrome	59.8	8.07	Xgboost, Booster: gblinear - Loss function: binary:logistic	500
Mental disease	60.4	9.18	SGDClassifier	200
Migraine	64.2	9.34	GradientBoostingClassifier	10000
Motion sickness	62.6	3.78	Xgboost, Booster: gblinear - Loss function: binary:hinge	100
Panic disorder	65.6	5.59	Xgboost, Booster: gblinear - Loss function: binary:logitraw	5000
Photic sneeze reflex photoptarmis	60.0	6.44	SGDClassifier	200
PTSD	74.0	23.02	Xgboost, Booster: gblinear - Loss function: binary:hinge	1000
Scoliosis	69.8	12.6	Xgboost, Booster: gblinear - Loss function: binary:logitraw	100
Sensitivity to Mosquito bites	61.0	13.51	Xgboost, Booster: gblinear - Loss function: binary:hinge	5000
Sleep disorders	68.4	18.64	SGDClassifier	200
Strabismus	67.8	12.66	SGDClassifier	1000
Thyroid issues cancer	76.0	13.87	Xgboost, Booster: gblinear - Loss function: binary:hinge	100
TypeIIDiabetes	69.6	15.65	PassiveAggressiveClassifier	500
Eczema	83.2	37.57	Xgboost, Booster: gbtree - Loss function: binary:hinge	100
Restless leg syndrome	66.0	17.68	AdaBoostClassifier	5000

Table 1. A table showing the best-performing machine learning algorithm in terms of AUC. The first column shows the phenotype, the second column shows the average AUC for five-fold, the third column shows the standard deviation, the fourth column shows the machine learning algorithm and hyperparameter that yielded the best performance for a particular phenotype, and the fifth column shows the number of SNPs yielding the best performance.

Phenotype	F1 Score	SD	Machine learning algorithm index	Number of SNPs
ADHD	45.4	8.26	SGDClassifier	1000
Allergicrhinitis	11.4	6.77	SGDClassifier	10000
Asthma	37.4	14.52	PassiveAggressiveClassifier	100
Bipolar disorder	88.0	6.71	ExtraTreesClassifier	500
Cholesterol	51.8	17.06	DecisionTreeClassifier	10000
Craves sugar	92.0	0.0	BaggingClassifier	200
Dental decay	90.0	0.0	BaggingClassifier	50
Depression	37.4	10.99	SGDClassifier	10000
Diagnosed vitamin D deficiency	38.0	14.88	SGDClassifier	1000
Diagnosed with sleep apnea	55.8	5.36	PassiveAggressiveClassifier	100
Dyslexia	30.0	1.87	SGDClassifier	10000
Earlobe free or attached	43.4	13.03	SGDClassifier	500
Hair type	38.0	17.39	SGDClassifier	100
Hypertension	91.0	8.22	ExtraTreesClassifier	5000
Hypertriglyceridemia	64.6	16.61	PassiveAggressiveClassifier	50
Irritable bowel syndrome	48.2	7.26	SGDClassifier	200
Mental disease	49.2	9.86	SGDClassifier	200
Migraine	71.2	2.39	RidgeClassifier	10000
Motion sickness	61.0	5.83	PassiveAggressiveClassifier	10000
Panic disorder	45.2	7.19	SGDClassifier	10000
Photoc sneeze reflex photoptarmis	61.0	6.4	SGDClassifier	200
PTSD	84.4	3.13	BaggingClassifier	500
Scoliosis	57.8	8.01	SGDClassifier	5000
Sensitivity to Mosquito bites	46.4	7.8	SGDClassifier	500
Sleep disorders	36.8	17.46	SGDClassifier	200
Strabismus	38.8	11.01	SGDClassifier	1000
Thyroid issues cancer	63.8	19.32	RidgeClassifier	100
TypeIIDiabetes	36.2	15.17	PassiveAggressiveClassifier	500
Eczema	71.2	27.88	DecisionTreeClassifier	500
Restless leg syndrome	46.0	28.81	AdaBoostClassifier	5000

Table 2. A table showing the best-performing machine learning algorithm in terms of F1-Score. The first column shows the phenotype, the second column shows the average F1-Score for five-folds, the third column shows the standard deviation, the fourth column shows the machine learning algorithm and hyperparameter that yielded the best performance for a particular phenotype, and the fifth column shows the number of SNPs yielding the best performance.

Phenotype	MCC	SD	Machine learning algorithm index	Number of SNPs
ADHD	12.2	14.52	SGDClassifier	500
Allergicrhinitis	0.0	0.0	AdaBoostClassifier	200
Asthma	15.6	24.58	PassiveAggressiveClassifier	100
Bipolar disorder	36.2	52.52	BaggingClassifier	10000
Cholesterol	25.6	30.92	DecisionTreeClassifier	10000
Craves sugar	31.8	37.42	PassiveAggressiveClassifier	50
Dental decay	24.8	13.86	PassiveAggressiveClassifier	500
Depression	22.6	10.85	DecisionTreeClassifier	50
Diagnosed vitamin D deficiency	13.2	29.52	BaggingClassifier	100
Diagnosed with sleep apnea	30.0	30.31	AdaBoostClassifier	500
Dyslexia	19.0	4.69	SGDClassifier	10000
Earlobe free or attached	29.6	29.57	RidgeClassifier	50
Hair type	25.6	14.31	BernoulliNB	10000
Hypertension	58.0	43.35	DecisionTreeClassifier	500
Hypertriglyceridemia	25.4	36.07	PassiveAggressiveClassifier	50
Irritable bowel syndrome	15.8	19.21	BernoulliNB	500
Mental disease	20.4	18.45	SGDClassifier	200
Migraine	29.0	18.75	GradientBoostingClassifier	10000
Motion sickness	23.8	22.88	SGDClassifier	200
Panic disorder	13.0	19.14	GradientBoostingClassifier	500
Photoc sneeze reflex photoptarmis	21.0	12.88	SGDClassifier	200
PTSD	12.8	28.62	BaggingClassifier	500
Scoliosis	32.2	54.17	RandomForestClassifier	100
Sensitivity to Mosquito bites	12.4	17.34	SGDClassifier	500
Sleep disorders	25.2	26.98	SGDClassifier	200
Strabismus	26.2	18.59	SGDClassifier	1000
Thyroid issues cancer	35.4	39.73	RidgeClassifier	100
TypeIIDiabetes	26.8	22.7	PassiveAggressiveClassifier	500
Eczema	52.2	51.5	DecisionTreeClassifier	500
Restless leg syndrome	30.4	33.78	AdaBoostClassifier	5000

Table 3. A table showing the best-performing machine learning algorithm in terms of MCC. The first column shows the phenotype, the second column shows the average MCC for five-folds, the third column shows the standard deviation, the fourth column shows the machine learning algorithm and hyperparameter that yielded the best performance for a particular phenotype, and the fifth column shows the number of SNPs yielding the best performance.

Phenotype	AUC	SD	Algorithm-Dropout-Optimizer-BatchSize-Epochs	Number of SNPs
ADHD	55.6	9.74	BILSTM-0.2-Adam-5-200	10000
Allergicrhinitis	67.4	5.86	ANN-0.2-Adam-5-50	500
Asthma	63.2	12.74	ANN-0.2-Adam-5-50	100
Bipolar disorder	73.0	14.82	GRU-0.2-Adam-5-200	50
Cholesterol	63.8	9.5	Stack GRU - BILSTM-0.2-Adam-1-200	10000
Craves sugar	78.0	26.12	GRU-0.5-Adam-5-50	100
Dental decay	72.0	4.47	Stack GRU - BILSTM-0.5-Adam-5-50	500
Depression	62.2	6.1	ANN-0.2-Adam-1-50	50
Diagnosed vitamin D deficiency	58.2	12.93	ANN-0.2-Adam-5-50	1000
Diagnosed with sleep apnea	66.4	7.8	LSTM-0.2-Adam-1-200	10000
Dyslexia	65.6	7.47	Stack LSTM - GRU-0.5-Adam-5-50	5000
Earlobe free or attached	64.6	8.08	BILSTM-0.5-Adam-1-50	5000
Hair type	58.8	8.81	Stack GRU - LSTM-0.2-Adam-1-50	1000
Hypertension	83.2	29.01	LSTM-0.2-Adam-1-50	10000
Hypertriglyceridemia	64.8	27.12	ANN-0.2-Adam-1-50	50
Irritable bowel syndrome	54.8	5.63	ANN-0.5-Adam-5-50	200
Mental disease	60.0	10.17	Stack LSTM - GRU-0.5-Adam-1-50	1000
Migraine	56.8	7.4	ANN-0.2-Adam-5-200	500
Motion sickness	59.6	8.59	ANN-0.5-Adam-5-200	5000
Panic disorder	57.4	10.88	Stack GRU - LSTM-0.5-Adam-5-200	5000
Photic sneeze reflex photoptarmis	65.8	8.41	Stack GRU - BILSTM-0.5-Adam-1-200	5000
PTSD	64.6	20.8	ANN-0.5-Adam-5-50	500
Scoliosis	69.6	22.74	ANN-0.5-Adam-1-200	100
Sensitivity to Mosquito bites	68.4	12.74	Stack LSTM - GRU-0.5-Adam-1-50	1000
Sleep disorders	66.8	11.65	Stack GRU - LSTM-0.5-Adam-1-200	100
Strabismus	71.0	11.07	ANN-0.2-Adam-1-50	500
Thyroid issues cancer	71.4	14.55	ANN-0.5-Adam-5-200	100
TypeIIDiabetes	78.6	13.67	Stack BILSTM - GRU-0.2-Adam-1-50	1000
Eczema	64.8	19.98	LSTM-0.5-Adam-1-200	50
Restless leg syndrome	54.8	24.0	ANN-0.2-Adam-5-200	5000

Table 4. A table showing the best-performing deep learning algorithm in terms of AUC. The first column shows the phenotype, the second column shows the average AUC for five-folds, the third column shows the standard deviation, the fourth column shows the deep learning algorithm and hyperparameter that yielded the best performance for a particular phenotype, and the fifth column shows the number of SNPs yielding the best performance.

Phenotype	F1 Score	SD	Algorithm-Dropout-Optimizer-BatchSize-Epochs	Number of SNPs
ADHD	40.6	8.38	ANN-0.5-Adam-1-200	200
Allergicrhinitis	18.2	2.86	ANN-0.2-Adam-5-50	500
Asthma	42.2	11.71	ANN-0.2-Adam-5-50	100
Bipolar disorder	77.4	10.41	Stack GRU - LSTM-0.2-Adam-1-200	5000
Cholesterol	53.6	17.34	ANN-0.2-Adam-5-200	200
Craves sugar	89.4	3.71	GRU-0.5-Adam-5-200	50
Dental decay	78.4	12.03	GRU-0.5-Adam-1-50	50
Depression	43.0	13.29	Stack LSTM - BILSTM-0.2-Adam-1-50	10000
Diagnosed vitamin D deficiency	39.6	6.07	Stack LSTM - GRU-0.5-Adam-5-50	10000
Diagnosed with sleep apnea	61.4	6.62	ANN-0.5-Adam-1-50	100
Dyslexia	36.8	16.16	GRU-0.5-Adam-5-50	10000
Earlobe free or attached	46.0	8.28	BILSTM-0.5-Adam-1-50	5000
Hair type	42.4	17.42	ANN-0.2-Adam-1-50	200
Hypertension	94.0	8.22	GRU-0.2-Adam-1-50	10000
Hypertriglyceridemia	67.8	23.86	ANN-0.2-Adam-1-50	50
Irritable bowel syndrome	51.6	5.32	ANN-0.2-Adam-1-200	10000
Mental disease	49.0	6.96	ANN-0.2-Adam-1-200	10000
Migraine	61.0	7.65	ANN-0.5-Adam-5-50	50
Motion sickness	65.4	5.27	ANN-0.5-Adam-5-200	5000
Panic disorder	49.8	8.04	ANN-0.5-Adam-1-200	10000
Photic sneeze reflex photoptarmis	64.4	10.88	Stack GRU - BILSTM-0.5-Adam-1-200	5000
PTSD	72.0	8.83	BILSTM-0.5-Adam-5-200	100
Scoliosis	67.2	23.86	ANN-0.5-Adam-1-200	100
Sensitivity to Mosquito bites	57.6	12.2	Stack LSTM - GRU-0.5-Adam-1-50	1000
Sleep disorders	34.4	9.07	Stack GRU - LSTM-0.5-Adam-1-200	100
Strabismus	43.0	30.36	Stack LSTM - GRU-0.2-Adam-1-200	50
Thyroid issues cancer	65.2	17.6	ANN-0.5-Adam-5-200	100
TypeIIDiabetes	48.6	20.84	Stack BILSTM - GRU-0.2-Adam-5-50	500
Eczema	60.2	11.48	ANN-0.5-Adam-5-50	10000
Restless leg syndrome	42.2	17.34	ANN-0.2-Adam-5-200	5000

Table 5. A table showing the best-performing deep learning algorithm in terms of F1-Score. The first column shows the phenotype, the second column shows the average F1-Score for five-folds, the third column shows the standard deviation, the fourth column shows the deep learning algorithm and hyperparameter that yielded the best performance for a particular phenotype, and the fifth column shows the number of SNPs yielding the best performance.

Phenotype	MCC	SD	Algorithm-Dropout-Optimizer-BatchSize-Epochs	Number of SNPs
ADHD	14.0	20.77	BILSTM-0.2-Adam-5-200	10000
Allergicrhinitis	18.6	4.62	ANN-0.2-Adam-5-50	500
Asthma	22.2	20.41	ANN-0.2-Adam-5-50	100
Bipolar disorder	40.8	25.06	GRU-0.2-Adam-5-200	50
Cholesterol	27.4	18.85	Stack GRU - BILSTM-0.2-Adam-1-200	10000
Craves sugar	46.6	45.5	GRU-0.5-Adam-5-50	100
Dental decay	35.6	18.23	Stack BILSTM - GRU-0.5-Adam-5-50	500
Depression	23.0	28.61	GRU-0.2-Adam-1-50	100
Diagnosed vitamin D deficiency	15.0	21.9	ANN-0.2-Adam-5-50	1000
Diagnosed with sleep apnea	34.0	16.03	LSTM-0.2-Adam-1-200	10000
Dyslexia	29.4	22.39	GRU-0.5-Adam-5-50	10000
Earlobe free or attached	25.4	14.05	BILSTM-0.5-Adam-1-50	5000
Hair type	23.4	22.66	Stack GRU - LSTM-0.2-Adam-1-50	1000
Hypertension	64.8	57.76	LSTM-0.2-Adam-1-50	10000
Hypertriglyceridemia	33.2	45.66	Stack GRU - LSTM-0.2-Adam-5-200	100
Irritable bowel syndrome	10.6	11.8	ANN-0.5-Adam-5-50	200
Mental disease	19.6	18.72	Stack LSTM - GRU-0.5-Adam-1-50	1000
Migraine	16.0	16.28	ANN-0.2-Adam-5-200	500
Motion sickness	20.8	17.38	ANN-0.5-Adam-5-200	5000
Panic disorder	16.0	20.68	Stack GRU - LSTM-0.5-Adam-5-200	5000
Photic sneeze reflex photoptarmis	33.0	16.12	Stack GRU - BILSTM-0.5-Adam-1-200	5000
PTSD	27.8	36.89	ANN-0.5-Adam-5-50	500
Scoliosis	41.2	44.67	ANN-0.5-Adam-1-200	100
Sensitivity to Mosquito bites	35.8	23.21	Stack LSTM - GRU-0.5-Adam-1-50	1000
Sleep disorders	23.4	14.42	Stack GRU - BILSTM-0.5-Adam-1-50	100
Strabismus	32.6	33.78	BILSTM-0.2-Adam-1-50	50
Thyroid issues cancer	46.6	28.83	ANN-0.5-Adam-5-200	100
TypeIIDiabetes	41.8	29.47	Stack BILSTM - GRU-0.2-Adam-5-50	500
Eczema	32.8	45.48	LSTM-0.5-Adam-1-200	50
Restless leg syndrome	6.6	29.33	ANN-0.5-Adam-1-200	5000

Table 6. A table showing the best-performing deep learning algorithm in terms of MCC. The first column shows the phenotype, the second column shows the average MCC for five-folds, the third column shows the standard deviation, the fourth column shows the deep learning algorithm and hyperparameter that yielded the best performance for a particular phenotype, and the fifth column shows the number of SNPs yielding the best performance.

Supplementary Material 3

This section lists the common genes identified by the machine and deep learning algorithms and those listed in the GWAS catalog for each phenotype.

ADHD

CUL3, LINC01965, TSNARE1, LRRN2, POC1B, RPL10AP3, PPP1R3B, POLR1H, PPP2R2B, NAV2, MYT1L, CCDC195, DUSP6, RPL6P5, SORCS3, ZMIZ1, TEX41

Allergicrhinitis

PRDM16, AKR1E2, LINC00705, IL1B

Asthma

MED24

Bipolardisorder

MRM2, PRKAG2, RNA5SP403, FOXN2, PPP1R21-DT, RNA5SP404, AHCYP3, RASIP1, "-", NCAN, SVEP1, TCF23

Cholesterol

Y_RNA, CUX1, CPLX3, RNU6-526P, RNU6-1151P, CEACAM16-AS1, PSRC1, SPOCK3, ABO, SH2B2, CDK6, TRIM31-AS1, SLC22A1, TOMM40, GDNF-AS1, GNAI3, NECTIN2, PPARA, ALDH1A2, RSRP1, RN7SL836P, NKPD1, CETP, GSK3B, MARK4, GIPR, FUT2, ULK3, LIPC-AS1, ABCG8, MPV17L2, LINC02117, CELSR2, LIPC, TRIM31, APOB, LITAF, MACO1

Cravessugar

No gene was identified.

Dentaldecay

CFH, PCDH9

Depression

Y_RNA, TMPRSS5, SNTN, ZP3P2, ZNF804A, LINC01977, STK19, "-", LINC02033, ZMIZ1, RNA5SP404, RNA5SP403, EHHADH-AS1, KLHDC8B, STK24, ITGA11, SMARCA2, CBX4, CPM, C3orf49, HOMER1, CSMD1, LINC01068, C3orf70, HSPD1P6, DRD2, TLL2, ARNTL, SNX4, ACTG1P22, RN7SL592P, VRK2, USP4

DiagnosedVitaminDdeficiency

ALDH1A2

DiagnosedwithSleepApnea

ACTN3

Dyslexia

FHIT

EarlobeFreeorattached

HairType

TCHH

Hypertension

ALDH1A2, GPR45, PRDM16, LINC02871, CYYR1-AS1, FIGN, MTHFR, PGAM1P5, TGFBRAP1, ATP2B1, FAT1P1, EML6, HIGD1AP3, PRPS1P1, SARM1, "-", MSX2, VTN

Hypertriglyceridemia

No gene was identified.

IrritableBowelSyndrome

No gene was identified.

MentalDisease

LINC02395, TMPRSS5, NTM, POC1B, CHN2, POM121L2, EXOC4, NGF-AS1, LINC01517, KCND2, FOXN2, IL1R2, CPVL, SCN2A, CNIH3, ZSCAN16-AS1, PSMA6P3, ITPRID1, PPP1R21-DT, NCKAP5, IL1R1, NEK6, OR12D3, FARP1, SPTLC1P2, NGF, LINC02151, LINC02326, RIN2, MSH5-SAPCD1, COL6A1, CSMD1, CLU, WDR7, MSH5, ADGRF5, DRD2, SGCG, HMGB1P46, OR5V1, DUSP6, LINC02674, ANK1, LHX2, ACTL8, HIP1

Migraine

No gene was identified.

LINC00645, ASTN2, MIR4307HG, NRP1, MARCHF4, BPIFC

Motionsickness

No gene was identified.

PanicDisorder

No gene was identified.

PhoticSneezeReflexPhotoptarmis

No gene was identified.

PosttraumaticStressDisorderorPTSD

No gene was identified.

Scoliosis

MAG1

SensitivitytoMosquitoBites

No gene was identified.

SleepDisorders

ASB3, MIR4431

Strabismus

No gene was identified.

ThyroidIssuesCancer

No gene was identified.

TypeIIDiabetes

MTNR1B, CDC123, IGF2BP2, SNRPGP16, KCNJ11, RN7SL198P

eczema

IL13, LINC01991, TH2LCRR, MSMB, BCL6

restlesslegsyndrome

BTBD9

References

1. Bastian Greshake, Philipp E. Bayer, Helge Rausch, and Julia Reda. openSNP—a crowdsourced web resource for personal genomics. *PLoS ONE*, 9(3):e89204, March 2014.
2. Muhammad Muneeb, Samuel F. Feng, and Andreas Henschel. Tutorial on 8 genotype files conversion. In *2022 10th International Conference on Bioinformatics and Computational Biology (ICBCB)*, pages 13–17, 2022.